# Enabling efficient high load ethanol-diesel dual-fuel combustion by Miller cycle and charge air cooling

Vinícius B. Pedrozo, Hua Zhao

Centre for Advanced Powertrain and Fuels Research (CAPF), Brunel University London, Kingston Lane, Uxbridge, Middlesex UB8 3PH, United Kingdom

* Corresponding author. E-mail address: vinicius.pedrozo@brunel.ac.uk (V. B. Pedrozo).

**Keywords**

Efficient dual-fuel combustion; ethanol; heavy-duty diesel engine; Miller cycle; HCCI; autoignition.

**Highlights**

- High net indicated efficiency was attained at 1.8 MPa IMEP.
- The maximum ethanol energy fraction was increased from 26% to 79% without EGR.
- NOx emissions were reduced by up to 57%.
- Miller cycle effectively delayed the ethanol autoignition process.
- A lower intake air temperature also curbed the early ignition of the ethanol fuel.

**Abstract**

Current dual-fuel engines often rely on the use of high levels of exhaust gas recirculation (EGR) to suppress excessive in-cylinder pressure rise rates (PRR) at high load conditions. This can increase the fuel economy penalty associated with the pumping losses on the boosting system of the engine. In this work, advanced combustion control strategies have been experimentally investigated to achieve efficient dual-fuel combustion at a high engine load 1.8 MPa net indicated mean effective pressure. The study assessed the potential of Miller cycle and charge air cooling to minimise the EGR requirements while maximising efficiency as well as the use of ethanol as a partial substitute for diesel fuel. Exhaust emissions and energy conversion efficiency were measured and discussed for different ethanol energy fractions. The experiments were carried out on a single-cylinder heavy-duty engine equipped with a high pressure common rail diesel injection, an ethanol port fuel injection, and a variable valve actuation system on the intake camshaft. The dual-fuel operation with a conventional valve timing resulted in an early autoignition of the premixed ethanol fuel and high levels of PRR, limiting the ethanol energy fraction to 26%. The introduction of a Miller cycle strategy via late intake valve closing events effectively delayed the autoignition process of ethanol. A reduction of 20 K in the inlet air temperature via an air-to-water charge air cooler also suppressed the early ignition of ethanol. As a result, ethanol-diesel dual-fuel combustion with Miller cycle and charge air cooling observed the potential to achieve high efficiencies without the need for EGR. Nitrogen oxides emissions were reduced in comparison with conventional diesel combustion. Moreover, a substantial improvement was attained in terms of the maximum ethanol energy fraction, which was increased to 79%.

## 1. Introduction

The vast majority of the transportation sector's energy needs is met by oil [1]. Increased global energy demand as well as greenhouse gas (GHG) emissions regulations are driving the use of renewable energy sources and advances in powertrain technology. The introduction of biofuels to efficient internal combustion engines can help reduce the transport sector's GHG emissions and petroleum dependence [2].

Biofuels are gaseous or liquid fuels produced from biomass, which is the biodegradable fraction of municipal and industrial waste as well as products, waste, and residues from agriculture, forestry, and related industries [3]. The life cycle GHG emissions for different biofuels [4] show that ethanol produced from sugar cane and wheat straw result in a significant lower carbon footprint than fossil fuels [5].

Dual-fuel combustion has been proven as an effective means of utilising alternative fuels in conventional diesel engines [6]. The combustion process is usually referred to Reactivity Controlled Compression Ignition (RCCI). This strategy can be achieved by the installation of a low cost port fuel injection system in the intake manifold for the formation of a low reactivity mixture of air and fuel, such as natural gas (NG), gasoline, or ethanol [7]. The stock diesel combustion and fuel injection systems can be retained in the dual-fuel engine. Direct injected diesel fuel serves as the ignition source for the premixed charge [8]. The use of different fuels as well as variations in the diesel injection timing and substitution ratio can change the dual-fuel combustion characteristics, emissions, and efficiencies.

Optimised dual-fuel combustion can attain lower nitrogen oxides (NOx) and soot emissions than conventional diesel combustion (CDC) [9,10]. Improvements in efficiency are also achievable [11,12]. However, relatively high levels of carbon monoxide (CO) and unburnt hydrocarbon (HC) emissions are usually reported at low engine loads [13]. Furthermore, engine operation at high

load conditions have been proved extremely challenging as a result of the peak in-cylinder pressure [14] and/or PRR limitations [15,16], which restrict the amount of low reactivity fuel used to very low percentages.

A number of studies have investigated combustion control strategies to allow for high load dual-fuel operation, such as the direct dual fuel stratification [17–19] or low temperature combustion [20–23]. However, these approaches often require relatively complex engine hardware modifications and/or high levels of EGR and boost pressure. Therefore, experimental research has been mostly focused on the use of a low compression ratio to decrease the in-cylinder gas pressure and temperature during the compression stroke. This delays the ignition of the fuel and allows for longer fuel-air mixing process [24].

The reduction in the compression ratio is typically attained via a modified piston [25]. High load gasoline-diesel dual-fuel combustion has been achieved on a medium-duty diesel engine using a piston with a lower geometric compression ratio (GCR) of 12.75:1 [26]. Despite the improvement, it is likely challenging to attain simultaneous high levels of boost pressure and EGR at a low intake charge temperature of 293 K in a production engine. In addition, experiments and computational optimisations performed on a heavy-duty engine with a GCR of 12:1 showed that controlling the dual-fuel combustion process at high loads can be a challenge due to the sensitivity to fluctuations in the EGR rate [27]. Furthermore, the introduction of a low GCR piston can lead to less efficient dual-fuel combustion at light loads [26].

Alternatively, the effective compression ratio (ECR) can be varied via an earlier or later intake valve closing event while retaining the stock piston and original compression ratio. The strategy is commonly known as Miller cycle and also reduces the in-cylinder charge temperature at the end of the compression stroke [28,29]. The approach allows for a more flexible combustion control if the valve timings can be varied according to engine operating condition. However, Miller cycle decreases the in-cylinder mass trapped at a constant intake manifold air pressure, which can

result in higher average combustion temperatures, increased heat transfer losses, and lower cycle efficiency [30].

Previous research with an early intake valve closing (EIVC) strategy has shown that gasoline-diesel dual-fuel combustion can be used over the entire engine speed-load map while maintaining the NOx emissions below 0.4 g/kWh [31]. The maximum engine load was increased from 1.2 MPa to 2.2 MPa break mean effective pressure (BMEP) when the ECR was reduced from 14.4:1 to 11:1. However, the study also relied on the use of high EGR rates, which likely placed a greater demand on the boosting system in order to supply enough air for lean and efficient engine operation.

The introduction of premixed fuels with high knock resistance such as ethanol and NG potentially allows for the use of relatively higher GCR/ECR's as well as lower EGR and boost requirements. The substitution of gasoline for a blend of 85% ethanol content in gasoline (E85) extended the dual-fuel operating range from 1.16 MPa to 1.9 MPa BMEP [32]. This was accomplished on a heavy-duty diesel engine with a GCR of 14:1 using an E85 mass fraction of 90% and an EGR rate of 41%. Goldsworthy [15] fumigated wet ethanol mixtures on a heavy-duty diesel engine with a GCR of 17.2:1. In this case, the experiments were carried out without EGR at high loads of 1.7 and 2.0 MPa BMEP. However, wet ethanol energy fractions were limited to approximately 30% due to rapid premixed combustion and excessive PRR's. Similarly, Hanson et al. [33] achieved 2.2 MPa BMEP using a NG mass fraction of 29% without the need for EGR. The experiments were performed at 1200 rpm on a heavy-duty diesel engine with a GCR higher than 17:1.

Although dual-fuel research has been carried out at high engine loads, most studies utilised gasoline and NG as a partial substitute for diesel fuel. In addition, the dual-fuel combustion strategies have required high levels of EGR to minimise PRR's, which can lead to fuel economy penalty due to pumping losses [21]. Previous investigations without EGR were limited to low premixed fuel fractions at such conditions.

Therefore, an experimental analysis has been performed to attain efficient high load dual-fuel combustion using the minimum EGR rate and the maximum ethanol energy fraction. Moreover, this is the first time that Miller cycle with late intake valve closing (LIVC) events and charge air cooling are systematically studied to improve the ethanol-diesel dual fuel combustion process at a high engine load.

The experiments were carried out on a heavy-duty diesel engine with a stock GCR of 16.8:1 at 1.8 MPa net indicated mean effective pressure (IMEP). The combustion characteristics, exhaust emissions, and fuel conversion efficiencies were compared for three ECR's of 16.8, 15.7, and 14.4:1 at different ethanol energy fractions. Similar experiments were performed to evaluate the effect of the intake manifold air temperature on high load ethanol-diesel dual-fuel combustion and emissions. The impact of varying the boost pressure and EGR rate on the combustion process was also revealed.

## 2. Experimental setup

### 2.1. Engine specifications and experimental facilities

A schematic diagram of the single cylinder heavy-duty engine experimental setup is shown in Figure 2. Fresh intake air was supplied to the engine via an external supercharger with closed loop for the boost pressure. A throttle located upstream of a large-volume surge tank provided fine control over the intake manifold air pressure. The air flow rate was measured with an

Endress+Hauser Proline t-mass 65F thermal mass flow meter. Another surge tank was installed in the exhaust manifold to damp out pressure fluctuations prior to the EGR circuit. An electronically controlled exhaust back pressure valve located downstream of the exhaust surge tank was used to set the required exhaust manifold pressure. The cooled external EGR was supplied to the engine intake system via an EGR valve. Boosted air and EGR temperatures were controlled using water cooled heat exchangers. Coolant and oil temperatures were kept at 353 ± 3 K. Oil pressure was set at 0.45 MPa throughout the experiments. Base hardware specifications are outlined in Table 1.

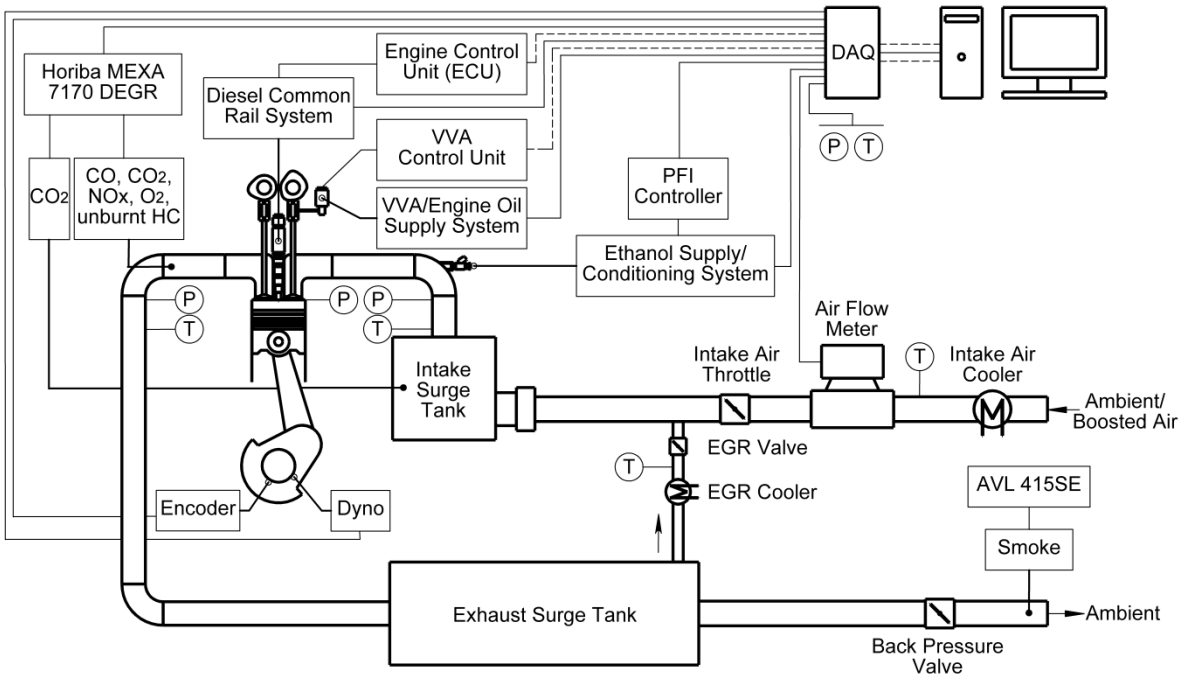


Figure 1 – Schematic diagram of the engine experimental setup.

Table 1 – Single cylinder heavy-duty diesel engine specifications.

| Parameter | Value |
|---|---|
| Displaced Volume | 2026 $cm^3$ |
| Stroke | 155 mm |
| Bore | 129 mm |
| Connecting Rod Length | 256 mm |
| Number of Valves | 4 |
| Piston Type | Re-entrant bowl |
| Geometric Compression Ratio | 16.8:1 |

| | |
|---|---|
| Maximum In-cylinder Pressure | 18 MPa |
| Diesel Injection System | Bosch common rail, injection pressure of 50–220 MPa, 8 holes with nominal diameter of 0.176 mm, included spray angle of 150° |
| Ethanol Injection System | PFI Marelli IWP069, included spray angle of 15° |

## 2.2. Fuel properties and delivery

Fuel properties are shown in Table 2. During dual-fuel operation, ethanol was injected through a port fuel injector (PFI). An injector driver controlled the PFI pulse width, adjusted according to the desired ethanol substitution ratio. The ethanol mass flow rate ($\dot{m}_{ethanol}$) was obtained from an injector calibration curve determined with a semi-microbalance with an accuracy of ± 0.1 mg. Ethanol injection pressure was continuously monitored, so that a constant relative pressure of 0.30 MPa could be maintained across the injector. A heat exchanger held the ethanol temperature at 295 ± 4 K.

Table 2 – Fuel properties.

| Property | Gasoil Ultra Low Sulphur | Anhydrous Ethanol |
|---|---|---|
| Density at 293 K ($\rho$) | 827 kg/m3 | 789 kg/m3 |
| Cetane Number | ~45 | - |
| RON [34] | - | ~107 |
| Alcohol Content | - | 99.1–99.5% (v/v) |
| Water Content | < 0.2 g/kg | < 1.14% (w/w) |
| Boiling Point/Range | 443-643 K | 351 K |
| Heat of Vaporisation [34] | 270 kJ/kg | 840 kJ/kg |
| Carbon Content | 86.6% | 52.1% |
| Hydrogen Content | 13.2% | 13.1% |
| Oxygen Content | 0.2% | 34.8% |
| Lower Heating Value (*LHV*) | 42.9 MJ/kg | 26.9 MJ/kg [34] |

The diesel fuel was supplied to the engine using a high pressure common rail injection system. The diesel injections were controlled via a dedicated engine control unit (ECU) with the ability to support up to three shots per cycle. Two Endress+Hauser Promass 83A Coriolis flow meters were used to determine the diesel flow rate ($\dot{m}_{diesel}$) by measuring the total fuel supplied to and from the high pressure pump and diesel injector.

The stoichiometric air/fuel ratio was determined by the conservation of mass of each chemical element in the reactants [34]. The global fuel-air equivalence ratio (Φ) was calculated using the intake air and fuel flow rates. The algorithm developed by Brettschneider-Spindt [35], which is based on the raw exhaust emissions, was used to confirm the results. The ethanol energy fraction (EF) varied from 0% to 79% during the experiments and was defined as

$$EF = \frac{\dot{m}_{ethanol}\, LHV_{ethanol}}{(\dot{m}_{ethanol}\, LHV_{ethanol}) + (\dot{m}_{diesel}\, LHV_{diesel})} \quad (1)$$

2.3. Exhaust measurements

Gaseous emissions such as CO, $CO_2$, NOx, $O_2$, and unburnt HC were taken using a Horiba MEXA-7170 DEGR gas analyser system. The EGR rate was calculated by the ratio of intake and exhaust $CO_2$ concentrations measured by the same analyser. The hydrocarbon emissions measured with its flame ionisation detector (FID) can lead to misinterpretation of unburnt HC trends as a result of the relative insensitivity of the equipment towards alcohols and aldehydes [36]. Therefore, the actual unburnt HC emissions were calculated using the method shown in [10]. An AVL 415SE smoke meter was used for soot emissions measurements. Combustion efficiency calculations were based on the emissions products not fully oxidised during the combustion process except soot by

$$Combustion\ Efficiency = 1 - \frac{(ISCO\ LHV_{CO}) + (ISHC\ LHV_{DF})}{(\dot{m}_{ethanol}\ LHV_{ethanol}) + (\dot{m}_{diesel}\ LHV_{diesel})}\ P_i \quad (2)$$

where ISCO and ISHC are the indicated specific emissions of CO and actual unburnt HC, respectively; $LHV_{CO}$ is equivalent to 10.1 MJ/kg; $P_i$ is the net indicated power; and $LHV_{DF}$ is the actual lower heating value for the in-cylinder fuel mixture in dual-fuel mode as

$$LHV_{DF} = \frac{(\dot{m}_{ethanol} LHV_{ethanol}) + (\dot{m}_{diesel} LHV_{diesel})}{\dot{m}_{ethanol} + \dot{m}_{diesel}} \quad (3)$$

2.4. Data analysis

The in-cylinder pressure was measured using a Kistler 6125C piezoelectric pressure sensor. Intake and exhaust pressures were measured with two Kistler 4049A water cooled piezoresistive absolute pressure sensors. The intake valve lift profile was continuously monitored by a LORD Microstrain linear differential variable reluctance transducer located on the top of the valve spring retainer. Two National Instruments data acquisition (DAQ) cards were used to acquire the signals from the measurement device. A high speed DAQ card received the crank angle resolved data synchronised with an optical encoder of 0.25 crank angle degrees (CAD) resolution. A lower speed DAQ card acquired the low frequency data, such as engine speed, torque, as well as temperatures and pressures at relevant locations. The data were calculated and displayed live by an in-house developed software.

Crank angle based in-cylinder pressure traces were averaged for 200 consecutive cycles for each operating point and used to calculate the IMEP and the apparent net heat release rate (HRR). Since the absolute value of the heat released is not as important to this study as the bulk shape of

the curve with respect to crank angle, a constant ratio of specific heats ($\gamma$) of 1.33 was assumed throughout the engine cycle. The mass fraction burnt (MFB) was calculated by integrating the HRR. Combustion phasing (CA50) was determined by the crank angle of 50% MFB.

The actual diesel injection timing (SOI) was determined from post-processing the current signal sent from the ECU to the injector solenoid. This signal was corrected by adding the energising time delay of 0.345 ms (e.g. ~2.5 CAD at 1200 rpm) measured in a constant volume chamber. Ignition delay was defined as the period of time between the actual start of main injection (SOI_main) and start of combustion (SOC), set to 0.3% MFB point of the average cycle.

The PRR represents the mean value of the maximum pressure rise rates of two-hundred un-filtered in-cylinder pressure cycles. Unless specifically noted, the average in-cylinder pressure and the resulting HRR were post-processed using a third order Savitzky-Golay filter with a window size of five data points. Cycle-to-cycle variability was measured by the coefficient of variation of IMEP (COV_IMEP) over the sampled cycles. Pumping mean effective pressure (PMEP) was calculated by the subtraction of the gross indicated mean effective pressure from the IMEP.

## 3. Methodology

### 3.1. Engine testing

Table 3 summarises the baseline engine operating conditions and highlights the optimised parameters. Testing was performed at a constant speed of 1200 rpm and a high engine load of 1.8 MPa IMEP. The maximum in-cylinder gas pressure (Pmax) and PPR were limited to 18 MPa and 2.0 MPa/CAD, respectively. The PRR limit was relaxed to 3.0 MPa/CAD on a few cases to allow for the determination of a given trend. The exhaust back pressure was varied when necessary to maintain a constant relative pressure to the intake manifold of 0.01 MPa and a comparable PMEP. Diesel fuel was introduced using a single injection near firing top dead centre (TDC). However, a

small pre-injection of an estimated volume of 3 $mm^3$ and a constant dwell time of 1 ms between pre- and main injection events was used in some conditions to minimise PRR's. The ethanol energy fraction and diesel injection timings were also varied when required. Stable engine operation was quantified by a COV_IMEP below 3%.

Table 3 – Engine operating conditions.

| Parameter | Baseline condition | Optimisation |
|---|---|---|
| Engine speed | 1200 rpm | |
| Load | 1.8 MPa IMEP | |
| Diesel injection pressure | 155 MPa | |
| Diesel injection strategy | Single | Pre-injection prior to the main |
| Ethanol energy fraction (EF) | 0% | Swept |
| Intake pressure | 0.26 MPa | Swept |
| Exhaust pressure | 0.27 MPa | Constant delta pressure of 0.01 MPa |
| EGR rate | 0% | Swept |
| EGR temperature | NA | 383 ± 3 K |
| Effective Compression Ratio (ECR) | 16:8:1 | Swept |
| Intake air temperature | 324 K | Swept |

### 3.2. Pressure-based effective compression ratio calculation

The engine features a variable valve actuation (VVA) system on the intake camshaft, incorporating a hydraulic tappet on the valve side of the rocker arm [37]. This system allows for the use of Miller cycle via modification of the intake valve closing (IVC) event as well as an intake valve re-opening during the exhaust stroke. Some experiments were carried out using the LIVC strategy, where the intake valve has been left open for longer than the baseline valve lift profile. This decreased the actual in-cylinder mass trapped as the piston expelled part of the inducted mass back into the intake port (reverse flow).

The later initiation of the compression process resulted in a lower ECR, which can be calculated as the ratio of the instantaneous in-cylinder volume at IVC (0.5 mm valve lift) to the clearance volume at TDC. However, this volume-based approach might not represent the actual

compression ratio due to the flow resistance across the intake valves [24] and inertia of the gas in the intake port before the inlet valves are closed [34].

Therefore, a pressure-based ECR calculation was employed in order to better account for the effect of the gas exchange process. The method uses the effective in-cylinder volume at IVC obtained from the intersection of an extrapolated polytropic compression curve and the average intake manifold pressure [24][30]. Figure 2 shows the determination of the effective volume at IVC (B), which resulted in a pressure-based ECR of 14.4:1. The use of the instantaneous volume at IVC (A) would lead to a volume-based ECR of 12.4:1.

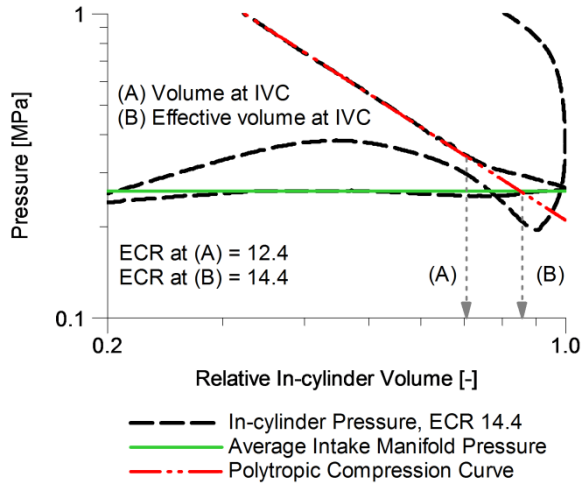


Figure 2 – In-cylinder pressure, average intake manifold pressure, and polytropic compression curve as a function of in-cylinder volume depicting the method used for computation of the volume-based (A) and pressure-based (B) ECR.

Figure 3 depicts the valve lift profiles used in this study to attain pressure-based ECR's of 16.8, 15.7, and 14.4:1. The intake valve opening (IVO) was set at 365 CAD after firing top dead centre (ATDC) as determined at 0.5 mm valve lift, maintaining the maximum lift constant. The expansion ratio also remained constant as a result of the fixed exhaust camshaft timing.

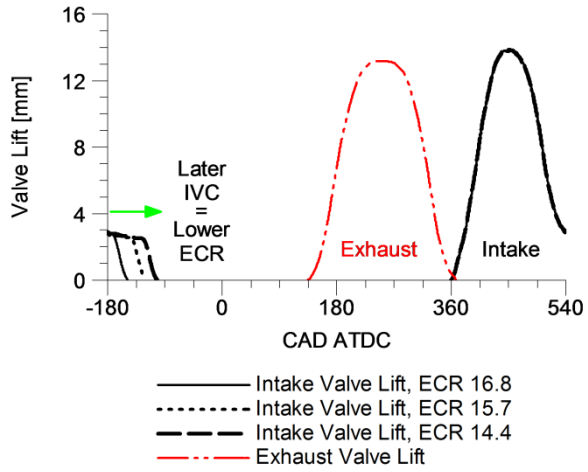


Figure 3 – Intake and exhaust valve lift profiles used in this study.

## 4. Results and Discussion

### 4.1. Early autoignition process of ethanol

Initially, experiments were performed to characterise the ethanol-diesel dual-fuel combustion with the default intake valve timings. The engine was operated using the baseline conditions showed in Table 3 with an ethanol energy fraction varied from 0% to 30%. The diesel injection timing was held constant at 4.75 CAD ATDC to ensure the premixed charge in the dual-fuel mode would contain only ethanol, air, and a small residual gas fraction (of approximately 3%). Any heat released prior to the SOI would be produced by the combustion of the ethanol fuel only.

Figure 4 shows that homogeneous charge compression ignition (HCCI) combustion of the ethanol fuel occurred prior to the start of the diesel injection. The premixed peak heat release increased with the ethanol content, reaching a PRR of 2.2 MPa/CAD at the substitution ratio of 30%. The increase in the total in-cylinder mass trapped and cooling effect introduced by higher ethanol energy fractions slightly reduced the maximum temperatures before TDC. However, the port fuel injected ethanol autoignited prior to the direct injection of diesel because of the high mean in-cylinder gas temperatures, which were above 950 K after -10 CAD ATDC.

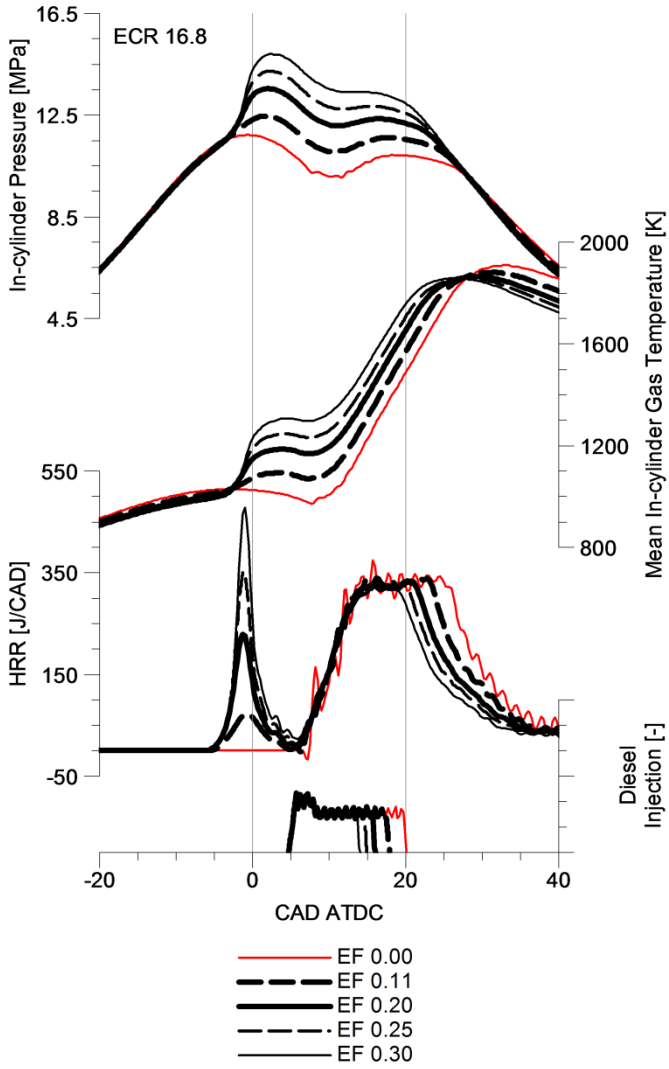


Figure 4 – In-cylinder pressure, mean in-cylinder gas temperature, HRR, and diesel injection timing for different ethanol energy fractions (EF) at an ECR of 16.8:1.

Fuel autoignition in internal combustion engines is predicted to take place between 900-950 K [38,39]. This is supported by Sjöberg and Dec's study [40], which revealed that the ethanol autoignition occurred as the mean in-cylinder gas temperature had reached more than 900 K. The ignition is followed by the production of water and heat release due to the reaction between hydroxyl (OH) radicals and fuel molecules [41]. The OH radicals are rapidly produced by the thermal decomposition of hydrogen peroxide ($H_2O_2$) as the in-cylinder gas temperature approaches the autoignition temperature. The $H_2O_2$ is formed and accumulated by low and intermediate temperature kinetic pathways during the compression stroke [38].

4.2. The effect of EGR

External EGR rate was varied from 0% to 21.1% in an attempt to delay the ethanol autoignition process. The exhaust and intake manifold air pressures were held constant. Figure 5 demonstrates that later SOC's and lower heat release peaks were attained as the EGR percentage was increased. In addition, the diesel mixing-controlled combustion became slower. However, reductions in the $O_2$ concentration and the higher heat capacity of the in-cylinder charge with EGR proved ineffective in mitigating the ethanol pre-ignition.

In a previous study by Sjöberg and Dec [40], it was shown that replacing inducted air with EGR and its different constituents could decrease the compression temperatures and slow down the intermediate-temperature heat-release rate (e.g. SOC-CA10) of the ethanol autoignition process. However, in the present study the early ignition of the ethanol fuel exhibited a relatively low sensitivity to variations in the in-cylinder $O_2$ concentration introduced by the actual engine EGR. This reduced sensitivity towards different levels of EGR can be partially attributed to the slightly higher intake charge temperature (2 K for 15.7% EGR, and 5 K for 21.2% EGR), as the recycled exhaust gas was hotter than boosted fresh air.

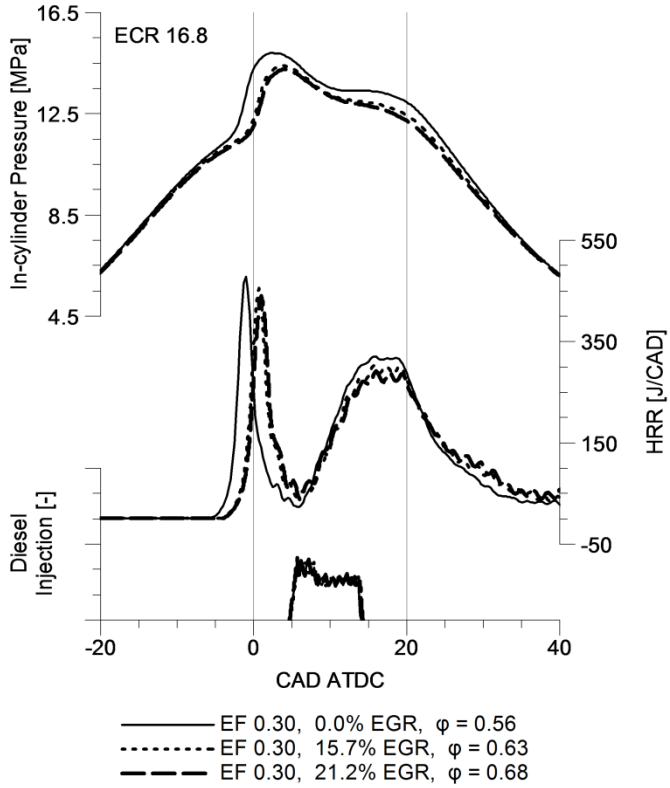


Figure 5 – In-cylinder pressure, HRR, and diesel injection timing for increased EGR rate using an ethanol energy fraction of 30%.

4.3. The effect of boost pressure

The relatively low EGR rates investigated in the previous section were considered ineffective in curbing the ethanol autoignition process. Therefore, intake manifold air pressure was varied from 0.24 MPa to 0.29 MPa to determine the effect of different global fuel-air equivalence ratios on the dual-fuel combustion. External EGR was not used and the exhaust manifold gas pressure was adjusted so as to maintain a constant relative pressure of 0.01 MPa to the intake runner for a similar PMEP.

Figure 6 shows that the autoignition of ethanol was practically unaffected as the boost pressure was swept. This was attributed to the similar compression temperatures, which were sufficiently high to ignite the premixed charge. An increase in the inlet air density reduced the global and premixed charge fuel-air equivalence ratios. The excess of air at highest boost pressure and

lowest Φ of 0.49 diluted the premixed charge and reduced the mean in-cylinder gas temperature as the combustion progressed. However, the increased $O_2$ availability led to a faster oxidation of the diesel fuel, as represented by the higher second peak heat release. In comparison, the use of a lower intake air pressure and a Φ of 0.62 resulted in a higher premixed peak heat release due the elevation of the in-cylinder gas temperatures during combustion.

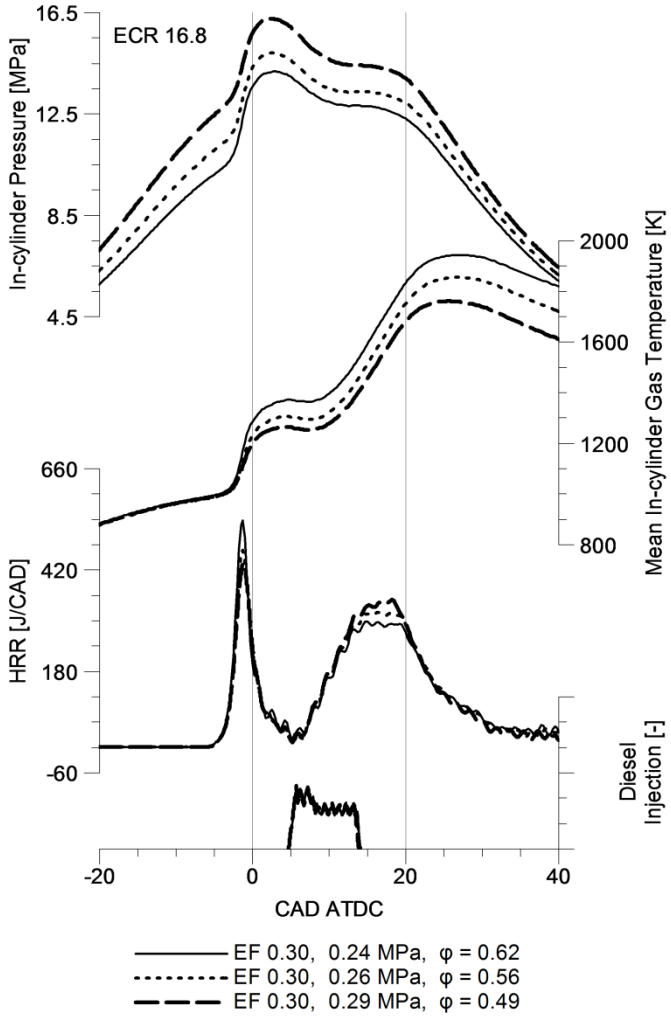


Figure 6 – In-cylinder pressure, mean in-cylinder gas temperature, HRR, and diesel injection timing for different intake manifold air pressures using an ethanol energy fraction of 30%.

4.4. The effect of ECR

The next approach studied aiming to eliminate the early ignition of ethanol and achieve efficient high load dual-fuel combustion was based on the use of Miller cycle via an LIVC strategy. The

sweep of ECR was initially performed for conventional diesel combustion and dual-fuel combustion with an ethanol energy fraction of 30%. The diesel injection timing was held at 4.75 CAD ATDC in the dual-fuel mode. The SOI used in CDC was advanced to approximately -4.25 CAD ATDC in order to minimise smoke. The intake manifold air pressure was held constant at 0.26 MPa.

Figure 7 depicts the effect of Miller cycle on the in-cylinder pressure, mean in-cylinder gas temperature, and resulting HRR. A reduction in the ECR decreased the in-cylinder charge density and pressure as well as the mean in-cylinder gas temperature during the compression stroke. In the CDC mode, the LIVC strategy resulted in longer mixing-controlled combustion. This is mainly attributed to a higher fuel-air equivalence ratio and thus a lower $O_2$ availability. Consequently, a higher amount of diesel fuel is burnt during the late combustion phase.

In the dual-fuel mode, a lower ECR successfully delayed the autoignition process of ethanol as a result of a lower mean in-cylinder gas temperature prior to the diesel SOI. The maximum gas temperature before the SOC dropped to less than 950 K at the latest IVC timing. Despite the improvement and the later SOC, the premixed charge was still auto-igniting just before the introduction of the diesel fuel. Engine experiments using an ECR lower than 14.4:1 was avoided and has not been shown due to high fuel economy penalty and misfire.

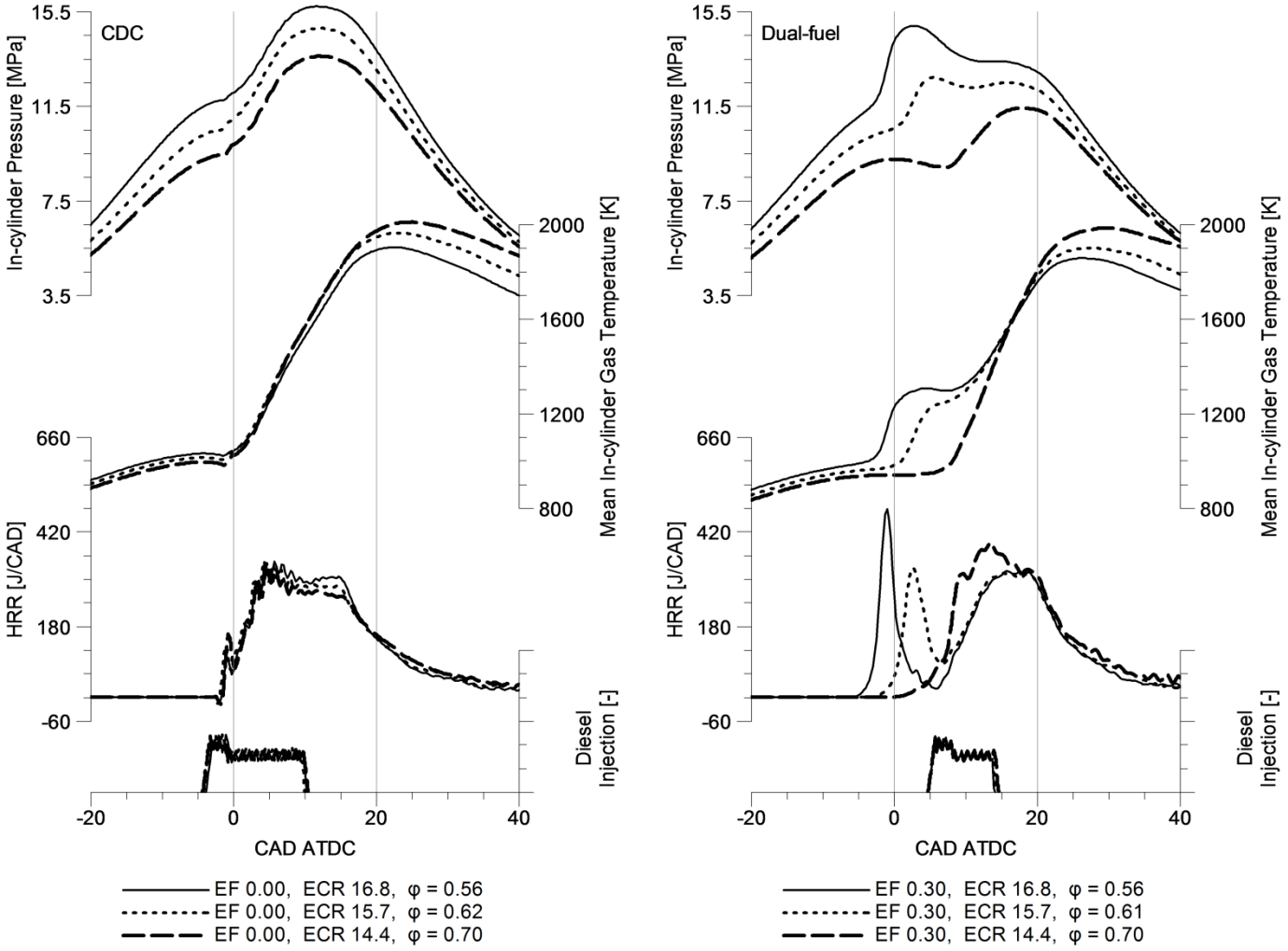


Figure 7 – In-cylinder pressure, mean in-cylinder gas temperature, HRR, and diesel injection timings for different ECR's in CDC and dual-fuel combustion modes.

4.5. High load dual-fuel operating range for different ECR's

The objective of this section was to map the ethanol-diesel dual-fuel operation with Miller cycle. The experiments were carried out without EGR while varying the ethanol energy fraction and diesel injection timings at different ECR's of 16.8, 15.7, and 14.4:1. The latest CA50 was limited to 16 CAD ATDC in order to minimise the fuel economy penalty.

Figure 8 shows that the dual-fuel operating range can be enlarged with lower ECR's. At an ECR of 16.8:1, the maximum ethanol percentage was PRR limited to 26% and the most advanced CA50 was at 8 CAD ATDC. The reduction of the ECR to 15.7:1 allowed for higher ethanol fractions of

40%. However, combustion phasing needed to be retarded because of the relatively longer ignition delays and higher PRR's. The use of a pre-injection of 3 $mm^3$ prior to the main diesel injection effectively lowered PRR's and was the key enabler for a more advanced and efficient dual-fuel combustion. Finally, the use of an ECR of 14.4:1 combined with a pre-injection of diesel substantially increased the maximum ethanol percentage to 79%. Peak in-cylinder pressure was only a concern for the most advanced cases performed with low ethanol energy fractions.

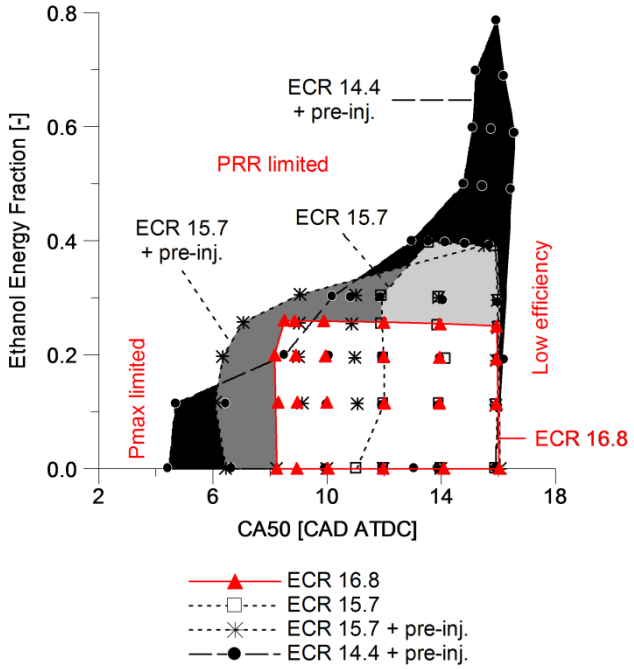


Figure 8 – Operating range for ethanol-diesel dual-fuel combustion using different ECR's and ethanol energy fractions at 1.8 MPa IMEP.

4.6. Combustion characteristics for different ECR's

Figure 9 depicts the SOI_main and the resulting heat release characteristics for the most efficient cases attained at each ECR and diesel injection strategy. The main diesel injection timing and combustion process were delayed as the ethanol percentage was increased in order to avoid excessive PRR. The operation at the lowest ECR of 14.4:1 was very sensitive to the start of injection. A slightly earlier injection resulted in PRR levels above the acceptable limit.

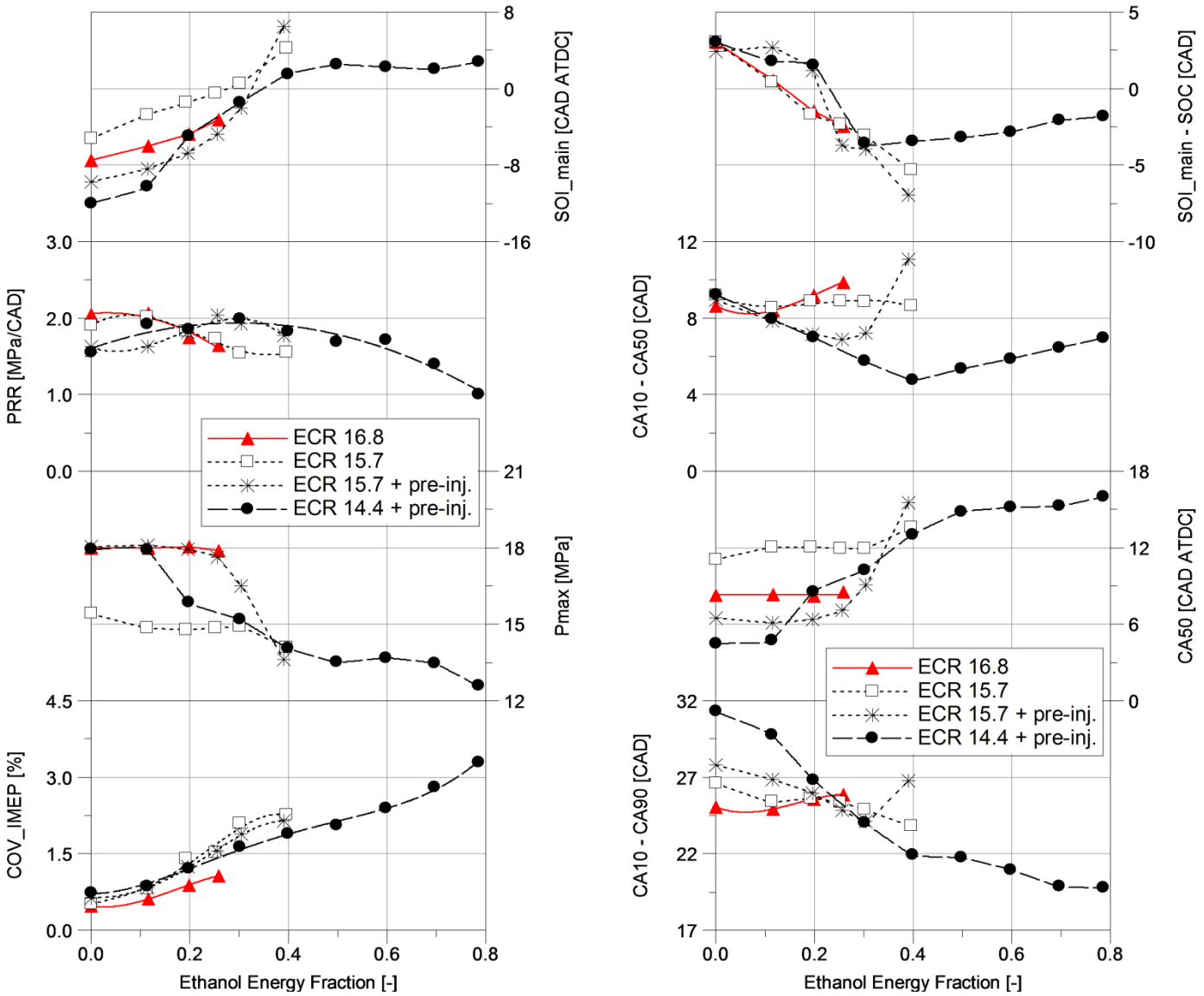


Figure 9 – Main diesel injection timings and the resulting heat release characteristics for the most efficient dual-fuel cases.

The later combustion process at high ethanol fractions lowered the peak in-cylinder pressure, as shown in Figures 9 and 10. The heat release profile usually changed from typical mixing-controlled combustion in CDC to a shorter combustion process with higher peak heat release in the dual-fuel mode. The introduction of higher amounts of premixed ethanol fuel increased the COV_IMEP, as revealed in Figure 9. Cycle-to-cycle variability was lower at the highest ECR of 16.8:1 as a result of the higher compression temperatures and probably more stable ignition of ethanol and diesel fuels.

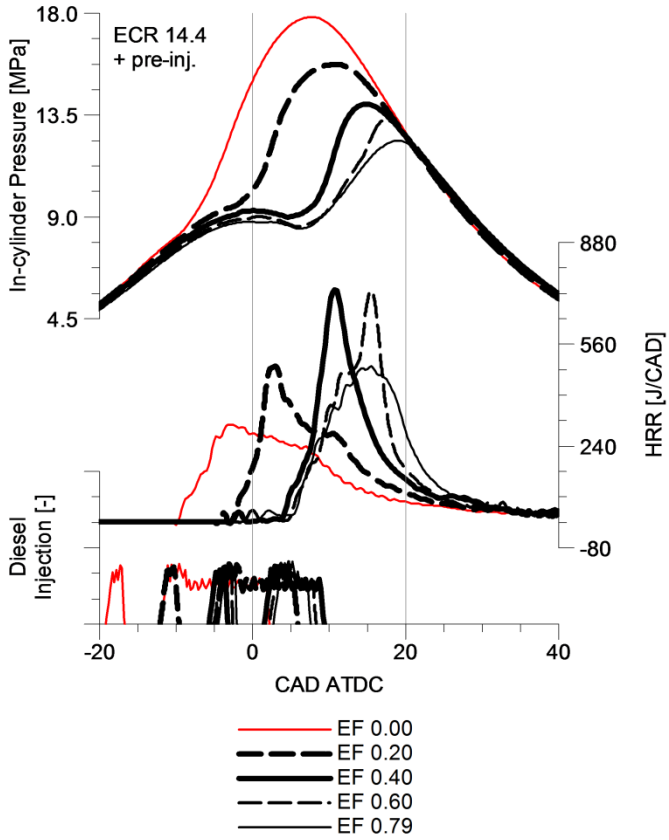


Figure 10 – In-cylinder pressure, HRR, and diesel injection timing for different ethanol energy fractions (EF) at an ECR of 14.4:1.

The period of time between the SOI_main and SOC in the dual-fuel mode remained below the interval measured for the diesel baseline cases. In addition, the ignition delay was shortened as the ethanol energy fraction was increased towards ~40%, as reported in [REF mid-load]. At the ECR of 14.4:1, the use of high substitution ratios (e.g. above 40%) led to relatively longer ignition delays due to the low reactivity of the ethanol fuel.

The first part of the heat release process between CA10 and CA50 was affected by the ECR, ethanol percentage, and diesel injection strategy. The most noticeable change was observed at the ECR of 14.4:1, where the CA10-CA50 period became shorter as the ethanol percentage was raised to 40%. This was probably caused by rapid simultaneous combustion of diesel and ethanol fuels. However, there was a reversal of the trend as the substitution ratio was further increased to 79% a result of charge cooling and slower reaction rates of the premixed fuel.

Despite the partial recovery of the first part of the combustion process between CA10 and CA50, the combustion phasing was held constant or retarded to avoid high PRR's. This is due to faster overall CA10-CA90 periods obtained at high ethanol energy fractions, especially at the ECR of 14.4:1. The exceptions occurred when more ethanol was used at the ECR of 16.8:1 and for an ethanol fraction of 39% with pre-injection of diesel at the ECR of 15.7:1. The slightly longer combustion duration in the first condition was mainly attributed to an earlier SOC caused by the ethanol fuel. In the second situation, the combustion process was extended as a result of the late diesel injection timing used to prevent the simultaneous combustion of the pre-injected diesel and premixed ethanol fuel.

### 4.7. Exhaust emissions and performance for different ECR's

Figure 11 shows the exhaust emissions, global fuel-air equivalence ratio, efficiencies, and fuel economy penalty for the optimum cases. The dual-fuel operation with a pre-injection of diesel and an ethanol energy fraction of 79% achieved 7.4 g/kWh of NOx at an ECR of 14.4:1. This is equivalent to an ISNOx reduction of 57% compared to the 17.3 g/kWh emitted by CDC at an ECR of 16.8:1. This improvement is a result of a later CA50 combined with a reduction in the amount of diesel fuel burnt during the mixing-controlled combustion phase. The use of an ECR of 15.7:1 emitted similar NOx levels to those attained at an ECR of 14.4:1 depending on the ethanol substitution ratio and diesel injection strategy.

The later injection and thus delayed combustion process attained at high ethanol percentages led to higher soot emissions. Lower in-cylinder gas temperatures and reduced oxygen concentration at such conditions are possibly linked to the elevation in the levels of smoke [42]. The highest ISsoot was 0.0024 g/kWh for an ethanol energy fraction of 79% at an ECR of 14.4:1, which is well below the Euro VI emission limit for particulate matter of 0.010 g/kWh [43].

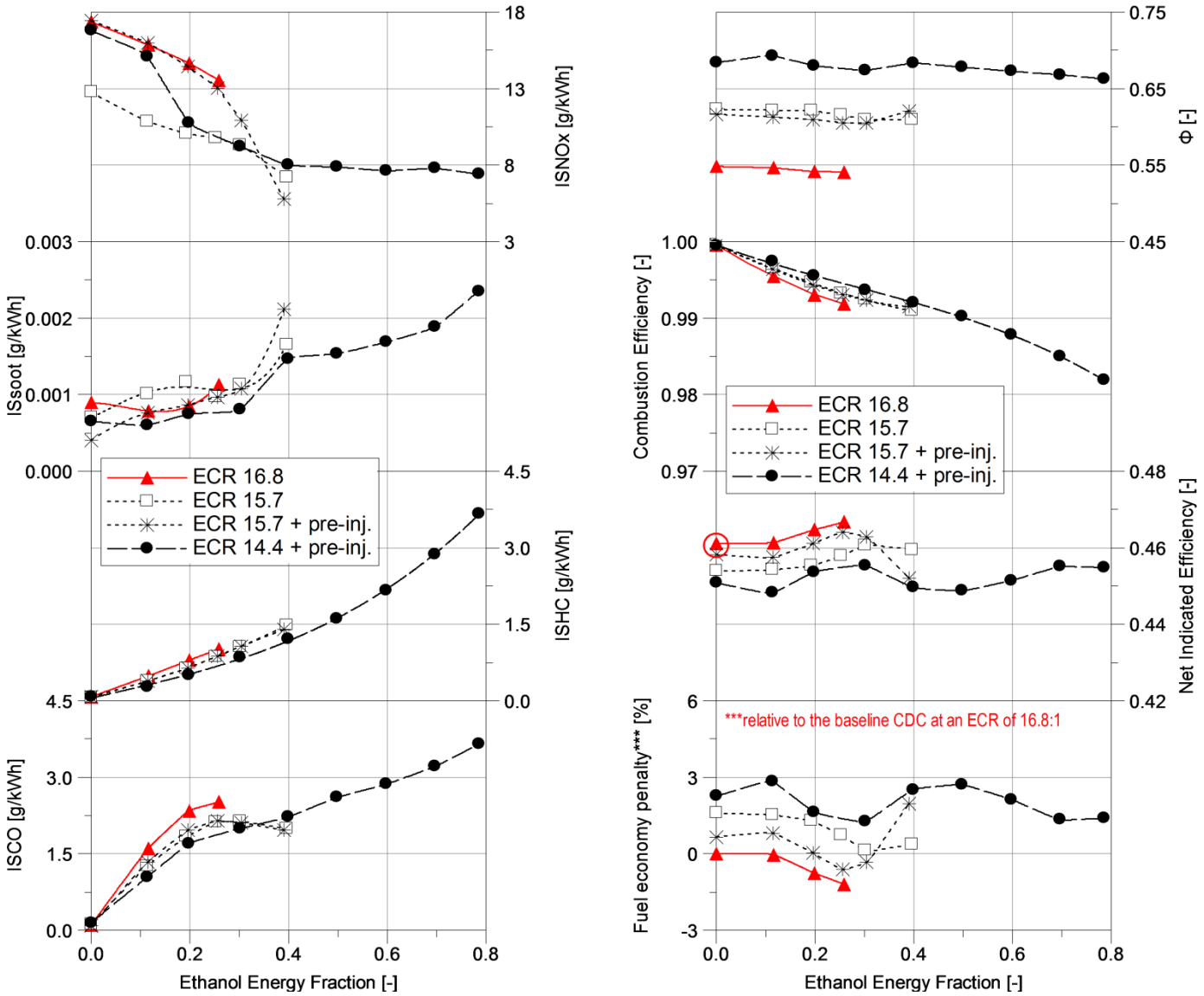


Figure 11 – Exhaust emissions and performance for the most efficient dual-fuel cases.

The CO and unburnt HC emissions increased as more ethanol was injected, reaching ~3.6 g/kWh at an ethanol energy fraction of 79%. This phenomenon occurs due to premixed fuel trapped in the crevice volumes of the stock diesel piston, as shown in the computational fluid dynamics modelling performed by Kokjohn et al. [44] and Desantes et al.[45]. The use of later IVC timings dropped the compression pressures, which possibly minimised the amount of ethanol fuel pushed into these crevice volumes. In addition, the adoption of a lower ECR increased the global fuel-air equivalence ratio and enhanced combustion process, allowing for higher combustion efficiencies.

The highest net indicated efficiency of 46.7% was attained with an ethanol substitution ratio of 26% at an ECR of 16.8:1. A reduction in the ECR at a constant intake manifold air pressure slightly decreased the net indicated efficiency. This was a result of a lower in-cylinder mass trapped and formation of a relatively richer mixture. A higher Φ reduced the ratio of specific heats and likely increased the heat transfer losses.

The resulting fuel economy penalty was calculated as

$$Fuel\ economy\ penalty\ [\%] = \left( \frac{\eta_{ind\ (CDC,\ \ ECR\ 16.8)} - \eta_{ind}}{\eta_{ind\ (CDC,\ \ ECR\ 16.8)}} \right) \times 100$$

where $\eta_{ind}$ is a given net indicated efficiency; and $\eta_{ind\ (CDC,\ \ ECR\ 16.8)}$ is the net indicated efficiency of 46.1% for the baseline CDC case at an ECR of 16.8:1 (red circle in Figure 11).

4.8. Efficient high load dual-fuel combustion enabled by Miller cycle

Figures 12 and 13 show the ISNOx and fuel economy penalty maps for different ethanol energy fractions and CA50 positions when operating the engine with an ECR of 14.4:1. The results demonstrate the trade-off between NOx emissions and efficiency as well as emphasise the potential of high load ethanol-diesel dual-fuel combustion. The optimised dual-fuel combustion process with an ethanol substitution ratio of 79% attained a net indicated efficiency of 45.45%. Compared to the diesel-only baseline at an ECR of 16.8:1, this was equivalent to a fuel economy penalty of only 1.4% for an ISNOx of 7.4 g/kWh. Alternatively, conventional diesel combustion would lead to a fuel economy penalty of 5.5% to achieve an ISNOx of 8.7 g/kWh. This analysis reveals the effectiveness of the alternative combustion mode in terms of NOx reduction and fuel conversion efficiency.

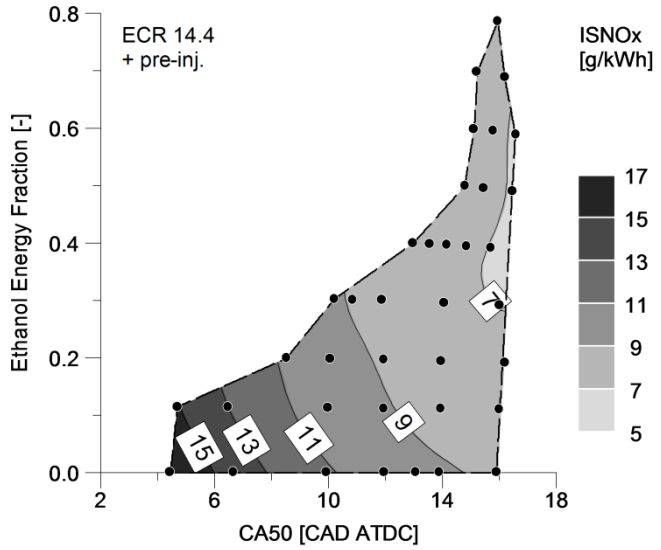


Figure 12 – ISNOx map for different ethanol energy fractions and CA50 positions.

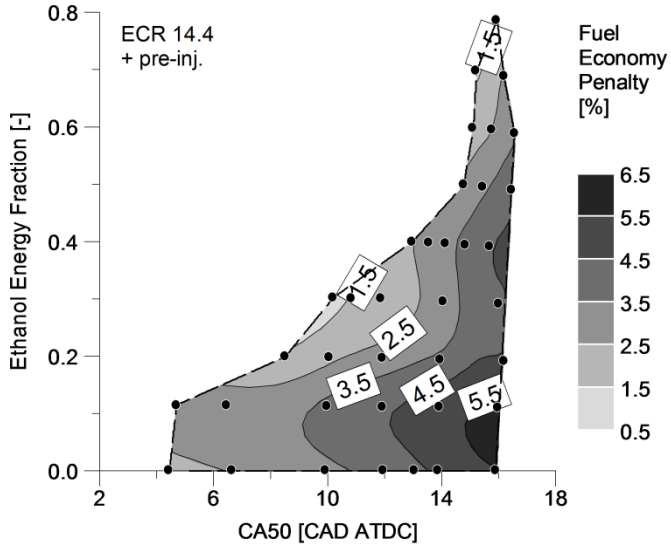


Figure 13 – Fuel economy penalty map for different ethanol energy fractions and CA50 positions.

4.9. The potential of charge air cooling

This section investigated whether a colder intake air is effective at delaying the ethanol autoignition process without EGR at an ECR of 16.8:1. The intake manifold air temperature was controlled using an air-to-water charge air cooler. The inlet pressure was held constant at 0.26 MPa. The ethanol energy fraction was set to 30% and the diesel injection timings were maintained at 4.75 CAD ATDC.

Figure 14 shows that a reduction in the intake manifold air temperature (IAT) from 324 K to 304 K decreased the mean in-cylinder gas temperature during the compression stroke and delayed the premixed fuel autoignition timing. The end-of-compression temperature and heat release process with a colder intake charge were comparable to the results attained with a higher IAT of 324 K at an ECR of 14.4:1. These similarities were attributed to the lower gas temperature and higher in-cylinder charge density at IVC for the case with an IAT of 304 K at an ECR of 16.8:1. This highlights the sensitivity of ethanol autoignition to variations in the in-cylinder gas temperature during the compression stroke, as the combustion of the premixed charge is mainly controlled by chemical kinetics [7].

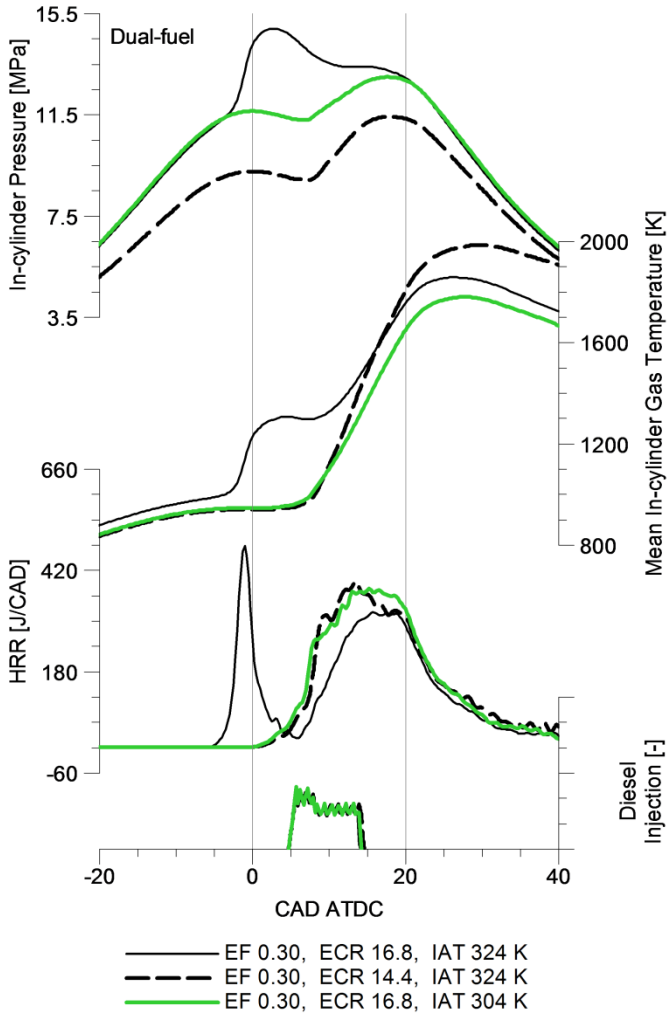


Figure 14 – In-cylinder pressure, mean in-cylinder gas temperature, HRR, and diesel injection timing for EF of 30% with different intake air temperatures at the ECR's of 16.8 and 14.4:1.

4.10. Efficient high load dual-fuel combustion enabled by charge air cooling

A one-off test was carried out with a higher ethanol energy fraction of 65% while maintaining an IAT of 304 K and an ECR of 16.8:1. The start of injection was optimised for the maximum net indicated efficiency. Figure 15 compares this result with the most efficient calibrations for ethanol energy fractions of 60% and 70% obtained with an IAT of 324 K at an ECR of 14.4:1. In all cases, a pre-injection of diesel was used to maintain the PRR within the limit of 2.0 MPa/CAD.

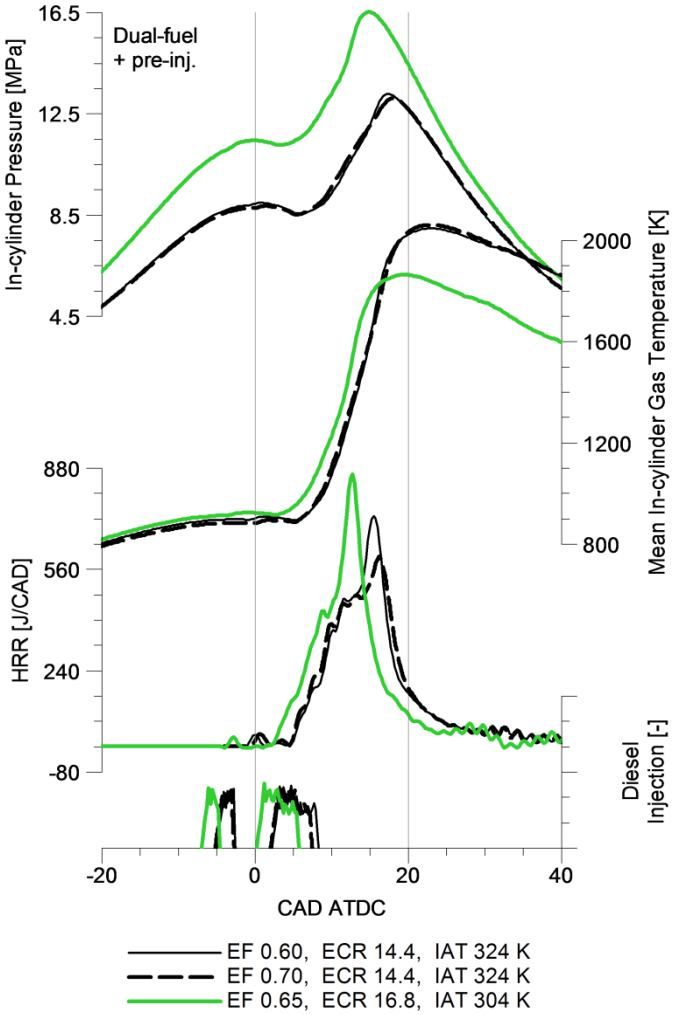


Figure 15 – In-cylinder pressure, mean in-cylinder gas temperature, HRR, and diesel injection timings for high EF's with different intake air temperatures at the ECR's of 16.8 and 14.4:1.

The colder inducted charge allowed for a similar although more advanced heat release than those at an ECR of 14.4:1. The leaner and earlier combustion process increased the net indicated efficiency from approximately 45.3% to 46.8%. The result represents an improvement of 1.5% relative to the net indicated efficiency of 46.1% obtained by the baseline CDC at an ECR of 16.8:1. However, higher $O_2$ availability somewhat minimised the NOx reduction benefit, leading to an ISNOx of 9.7 g/kWh. In addition, the lower Φ decreased the combustion efficiency to 96.6%. Further analyses were not performed as low intake air temperatures might not be achievable from a practical standpoint. Unacceptable PRR levels can possibly be experienced when using hotter intake air charges or running the engine at higher loads (e.g. 2.4 MPa IMEP).

## 5. Conclusions

In this study, engine experiments were performed to attain optimised ethanol-diesel dual-fuel combustion at a high load condition of 1.8 MPa IMEP. Advanced combustion strategies were evaluated to maximise the ethanol energy fraction and minimise the fuel economy penalty associated with the use of high EGR rates. The potential of Miller cycle via late intake valve closing events and charge air cooling via an air-to-water heat exchanger was explored. The effect of ethanol percentage, EGR rate, and intake manifold air pressure on the combustion process was also analysed. The combustion characteristics, exhaust emissions, and efficiencies were discussed. The investigation was carried out on a single cylinder heavy-duty diesel engine with a geometric compression ratio of 16.8:1. The primary findings can be summarised as follows:

- High pressure rise rates were observed as the ethanol percentage was increased at the baseline effective compression ratio of 16.8:1. This was a result of the early autoignition process of the premixed charge, which limited the maximum ethanol energy fraction to 26%.
- Changes the global fuel-air equivalence ratio via different boost levels did not curb the pre-ignition of ethanol.

- The introduction of EGR rates of 15.7% and 21.1% was not effective in mitigating the ethanol compression ignition prior to the diesel injection.
- The application of Miller cycle via LIVC events reduced the ECR to 15.7:1 and 14.4:1. This delayed the premixed charge autoignition timing and decreased the levels of PRR.
- The engine operation with a split diesel injection strategy (pre- and main) combined to an ECR of 14.4:1 allowed for the use of more advanced burn rates and ethanol substitution ratios up to 79%.
- Optimised ethanol-diesel dual-fuel combustion with Miller cycle (ECR of 14.4:1) attained a fuel economy penalty of only 1.4% for 57% lower NOx emissions than the baseline diesel combustion at an ECR of 16.8:1.
- The reduction of the intake air temperature via a charge air cooler effectively decreased the compression temperatures, suppressing the early autoignition of ethanol at an ECR of 16.8:1. The resulting heat release rates were similar to those achieved with a 20 K higher inlet air temperature at an ECR of 14.4:1.
- The use of charge air cooling at an ECR of 16.8:1 recovered the fuel economy penalty observed with Miller cycle. This emphasises the importance of intake air temperature control for high efficiency dual-fuel combustion.

Ethanol-diesel dual-fuel combustion offers potential to reduce the oil dependence as well as mitigate GHG emissions by the diversification of the fuel energy supply and use of a low carbon fuel. The results highlighted the sensitivity of ethanol autoignition to variations in the mean in-cylinder gas temperature. In addition, the study demonstrated the potential of Miller cycle and charge air cooling to enable efficient high load dual-fuel engine operation without EGR. Challenges will still remain on the effectiveness of Miller cycle and charge air cooling at full engine load (2.4 MPa IMEP).

**Acknowledgments**

V. Pedrozo would like to acknowledge CAPES Foundation – Ministry of Education of Brazil for supporting his PhD study at Brunel University London under supervision of Prof. Zhao.

**Glossary**

ATDC, After Firing Top Dead Centre; BMEP, Break Mean Effective Pressure; CA10, Crank Angle of 10% Cumulative Heat Release; CA10-CA50, 10-50% Cumulative Heat Release; CA10-CA90, Combustion Duration or 10-90% Cumulative Heat Release; CA50, Crank Angle of 50% Cumulative Heat Release; CA90, Crank Angle of 90% Cumulative Heat Release; CAD, Crank Angle Degrees; CDC, Conventional Diesel Combustion; CO, Carbon Monoxide; $CO_2$, Carbon Dioxide; COV_IMEP, Coefficient of Variation of IMEP; DAQ, Data Acquisition; DF, Dual-Fuel; E85, Gasoline with 85% Ethanol in a Volume Basis; ECR, Effective Compression Ratio; ECU, Engine Control Unit; EF, Ethanol Energy Fraction; EGR, Exhaust Gas Recirculation; EIVC, Early Intake Valve Closing; FID, Flame Ionisation Detector; GCR, Geometric Compression Ratio; GHG, Greenhouse Gas; HC, Hydrocarbons; HRR, Apparent Net Heat Release Rate; IAT, Intake Manifold Air Temperature; IMEP, Net Indicated Mean Effective Pressure; ISCO, Net Indicated Specific Emissions of CO; ISHC, Net Indicated Specific Emissions of the Actual Unburnt HC; ISNOx, Net Indicated Specific Emissions of NOx; ISsoot, Net Indicated Specific Emissions of Soot; IVC, Intake Valve Closing; IVO, Intake Valve Opening; $LHV_{CO}$, Lower Heating Value of Carbon Monoxide; $LHV_{DF}$, Actual Lower Heating Value in Dual-Fuel Mode; $LHV_{diesel}$, Lower Heating Value of Diesel; $LHV_{ethanol}$, Lower Heating Value of Ethanol; LIVC, Late Intake Valve Closing; $\dot{m}_{diesel}$, Mass Flow Rate of Diesel; $\dot{m}_{ethanol}$, Mass Flow Rate of Ethanol; MFB, Mass Fraction Burnt; NG, Natural Gas; NOx, Nitrogen Oxides; $O_2$, Oxygen; $P_i$, Net Indicated Power; PFI, Port Fuel Injector; Pmax, Maximum In-cylinder Gas Pressure; PMEP, Pumping Mean Effective Pressure; PRR, Pressure Rise Rate; SOC, Start of Combustion; SOI, Actual Diesel Injection Timing; SOI_main,

Actual Start of Main Injection; TDC, Firing Top Dead Centre; VVA, Variable Valve Actuation; $\gamma$, Ratio of Specific Heats; Φ, Global Fuel-Air Equivalence Ratio.

**References**


[1] Exxon Mobil Corporation. 2017 Outlook for Energy: A View to 2040. Irving, Texas: 2017.

[2] European Commission. Clean Transport - Support to the Member States for the Implementation of the Directive on the Deployment of Alternative Fuels Infrastructure: Good Practice Examples 2016.

[3] European Parliament and of the Council. Directive 2003/30/EC of the European Parliament and of the Council. Official Journal of the European Union 2003;123.

[4] European Parliament and of the Council. Directive 2009/28/EC of the European Parliament and of the Council. Official Journal of the European Union 2009;140.

[5] European Parliament and of the Council. Directive 2015/652 of the European Parliament and of the Council. Official Journal of the European Union 2015;107.

[6] Reitz RD. Directions in internal combustion engine research. Combustion and Flame 2013;160:1–8. doi:10.1016/j.combustflame.2012.11.002.

[7] Reitz RD, Duraisamy G. Review of high efficiency and clean reactivity controlled compression ignition (RCCI) combustion in internal combustion engines. Progress in Energy and Combustion Science 2015;46:12–71. doi:10.1016/j.pecs.2014.05.003.

[8] Li J, Yang W, Zhou D. Review on the management of RCCI engines. Renewable and Sustainable Energy Reviews 2017;69:65–79. doi:10.1016/j.rser.2016.11.159.

[9] Pedrozo VB, May I, Dalla Nora M, Cairns A, Zhao H. Experimental analysis of ethanol dual-fuel combustion in a heavy-duty diesel engine: An optimisation at low load. Applied Energy 2016;165:166–82. doi:10.1016/j.apenergy.2015.12.052.

[10] Pedrozo VB, May I, Lanzanova TDM, Zhao H. Potential of internal EGR and throttled operation for low load extension of ethanol–diesel dual-fuel reactivity controlled compression ignition combustion on a heavy-duty engine. Fuel 2016;179:391–405. doi:10.1016/j.fuel.2016.03.090.

[11] Pedrozo V, May I, Zhao H. Characterization of Low Load Ethanol Dual-Fuel Combustion using Single and Split Diesel Injections on a Heavy-Duty Engine. SAE Technical Paper 2016. doi:10.4271/2016-01-0778.

[12] Molina S, García a., Pastor JM, Belarte E, Balloul I. Operating range extension of RCCI combustion concept from low to full load in a heavy-duty engine. Applied Energy 2015;143:211–27. doi:10.1016/j.apenergy.2015.01.035.

[13] Wang Y, Yao M, Li T, Zhang W, Zheng Z. A parametric study for enabling reactivity controlled compression ignition (RCCI) operation in diesel engines at various engine loads. Applied Energy 2016;175:389–402. doi:10.1016/j.apenergy.2016.04.095.

[14] May I, Pedrozo V, Zhao H, Cairns A, Whelan S, Wong H, et al. Characterization and Potential of Premixed Dual-Fuel Combustion in a Heavy Duty Natural Gas/Diesel Engine. SAE Technical Paper 2016. doi:10.4271/2016-01-0790.

[15] Goldsworthy L. Fumigation of a heavy duty common rail marine diesel engine with ethanol-water mixtures. Experimental Thermal and Fluid Science 2013;47:48–59. doi:10.1016/j.expthermflusci.2012.12.018.

[16] Benajes J, García A, Monsalve-Serrano J, Balloul I, Pradel G. An assessment of the dual-mode reactivity controlled compression ignition/conventional diesel combustion capabilities

in a EURO VI medium-duty diesel engine fueled with an intermediate ethanol-gasoline blend and biodiesel. Energy Conversion and Management 2016;123:381–91. doi:10.1016/j.enconman.2016.06.059.

[17] Lim JH, Reitz RD. High Load (21 Bar IMEP) Dual Fuel RCCI Combustion Using Dual Direct Injection. Journal of Engineering for Gas Turbines and Power 2014;136. doi:10.1115/1.4027361.

[18] Wissink M, Reitz RD. Direct Dual Fuel Stratification, a Path to Combine the Benefits of RCCI and PPC. SAE International Journal of Engines 2015;8:878–89. doi:10.4271/2015-01-0856.

[19] Wissink M, Reitz R. Exploring the Role of Reactivity Gradients in Direct Dual Fuel Stratification. SAE International Journal of Engines 2016;9:2016–01 – 0774. doi:10.4271/2016-01-0774.

[20] Wu Y, Reitz RD. Effects of Exhaust Gas Recirculation and Boost Pressure on Reactivity Controlled Compression Ignition Engine at High Load Operating Conditions. Journal of Energy Resources Technology 2015;137. doi:10.1115/1.4029866.

[21] Kavuri C, Kokjohn S. Investigating Air Handling Requirements of High Load Low Speed Reactivity Controlled Compression Ignition (RCCI) Combustion. SAE Technical Paper 2016. doi:10.4271/2016-01-0782.

[22] Han X, Divekar P, Reader G, Zheng M, Tjong J. Active Injection Control for Enabling Clean Combustion in Ethanol-Diesel Dual-Fuel Mode. SAE International Journal of Engines 2015;8:890–902. doi:10.4271/2015-01-0858.

[23] Han X, Zheng M, Tjong J. Clean combustion enabling with ethanol on a dual-fuel compression ignition engine. International Journal of Engine Research 2015:1–13. doi:10.1177/1468087415575646.

[24] He X, Durrett RP, Sun Z. Late Intake Valve Closing as an Emissions Control Strategy at Tier 2 Bin 5 Engine-Out NOx Level. SAE International Journal of Engines 2008;1:2008–01 – 0637. doi:10.4271/2008-01-0637.

[25] Benajes J, García A, Monsalve-Serrano J, Boronat V. Achieving clean and efficient engine operation up to full load by combining optimized RCCI and dual-fuel diesel-gasoline combustion strategies. Energy Conversion and Management 2017;136:142–51. doi:10.1016/j.enconman.2017.01.010.

[26] Benajes J, Pastor J V., García A, Boronat V. A RCCI operational limits assessment in a medium duty compression ignition engine using an adapted compression ratio. Energy Conversion and Management 2016;126:497–508. doi:10.1016/j.enconman.2016.08.023.

[27] Kavuri C, Paz J, Kokjohn SL. A comparison of Reactivity Controlled Compression Ignition (RCCI) and Gasoline Compression Ignition (GCI) strategies at high load, low speed conditions. Energy Conversion and Management 2016;127:324–41. doi:10.1016/j.enconman.2016.09.026.

[28] Martins MES, Lanzanova TDM. Full-load Miller cycle with ethanol and EGR: Potential benefits and challenges. Applied Thermal Engineering 2015;90:274–85. doi:10.1016/j.applthermaleng.2015.06.086.

[29] Zhao J. Research and application of over-expansion cycle (Atkinson and Miller) engines – A review. Applied Energy 2017;185:300–19. doi:10.1016/j.apenergy.2016.10.063.

[30] Ickes A, Hanson R, Wallner T. Impact of Effective Compression Ratio on Gasoline-Diesel Dual-Fuel Combustion in a Heavy-Duty Engine Using Variable Valve Actuation. SAE Technical Paper 2015. doi:10.4271/2015-01-1796.

[31] Benajes J, Pastor J V., García A, Monsalve-Serrano J. The potential of RCCI concept to meet EURO VI NOx limitation and ultra-low soot emissions in a heavy-duty engine over the whole engine map. Fuel 2015;159:952–61. doi:10.1016/j.fuel.2015.07.064.

[32] Zhang Y, Sagalovich I, De Ojeda W, Ickes A, Wallner T, Wickman DD. Development of Dual-Fuel Low Temperature Combustion Strategy in a Multi-Cylinder Heavy-Duty Compression Ignition Engine Using Conventional and Alternative Fuels. SAE International Journal of Engines 2013;01:1481–9. doi:10.4271/2013-01-2422.

[33] Hanson R, Ickes A, Wallner T. Use of Adaptive Injection Strategies to Increase the Full Load Limit of RCCI Operation. Journal of Engineering for Gas Turbines and Power 2016;138:102802. doi:10.1115/1.4032847.

[34] Heywood JB. Internal Combustion Engine Fundamentals. 1st ed. McGraw-Hill, Inc.; 1988.

[35] Silvis WM. An Algorithm for Calculating the Air/Fuel Ratio from Exhaust Emissions. SAE Technical Paper 1997. doi:10.4271/970514.

[36] Wallner T. Correlation Between Speciated Hydrocarbon Emissions and Flame Ionization Detector Response for Gasoline/Alcohol Blends. Journal of Engineering for Gas Turbines and Power 2011;133. doi:10.1115/1.4002893.

[37] Schwoerer J, Kumar K, Ruggiero B, Swanbon B. Lost-Motion VVA Systems for Enabling Next Generation Diesel Engine Efficiency and After-Treatment Optimization. SAE Technical Paper 2010. doi:10.4271/2010-01-1189.

[38] Westbrook CK. Chemical kinetics of hydrocarbon ignition in practical combustion systems. Proceedings of the Combustion Institute 2000;28:1563–77. doi:10.1016/S0082-0784(00)80554-8.

[39] Westbrook CK, Pitz WJ, Leppard WR. The Autoignition Chemistry of Paraffinic Fuels and Pro-Knock and Anti-Knock Additives: A Detailed Chemical Kinetic Study. SAE Technical Paper 1991. doi:10.4271/912314.

[40] Sjöberg M, Dec JE. Effects of EGR and its constituents on HCCI autoignition of ethanol. Proceedings of the Combustion Institute 2011;33:3031–8. doi:10.1016/j.proci.2010.06.043.

[41] Aceves SM, Flowers DL, Martinez-Frias J, Smith JR, Dibble R, Au M, et al. HCCI Combustion: Analysis and Experiments. SAE Technical Paper 2001. doi:10.4271/2001-01-2077.

[42] Benajes J, Molina S, Martín J, Novella R. Effect of advancing the closing angle of the intake valves on diffusion-controlled combustion in a HD diesel engine. Applied Thermal Engineering 2009;29:1947–54. doi:10.1016/j.applthermaleng.2008.09.014.

[43] European Parliament and of the Council. Commission Regulation (EU) No 582/2011. Official Journal of the European Union 2011;167.

[44] Kokjohn SL, Hanson RM, Splitter D a, Reitz RD. Fuel reactivity controlled compression ignition (RCCI): a pathway to controlled high-efficiency clean combustion. International Journal of Engine Research 2011;12:209–26. doi:10.1177/1468087411401548.

[45] Desantes JM, Benajes J, García A, Monsalve-Serrano J. The role of the in-cylinder gas temperature and oxygen concentration over low load reactivity controlled compression ignition combustion efficiency. Energy 2014;78:854–68. doi:10.1016/j.energy.2014.10.080.